The AC losses measurement and analysis of superconducting NbTi CICC for HT-TU superconducting Tokamak

FANG Jin[1], WENG Pei-De[2], CHEN Zhuo-Min[2], CHEN Jing-Lin[2], WANG Fu-Tang[2], HAN Zheng-He[1]

([1]Applied Superconductivity Research Center, Tsinghua University, Beijing 100084; [2]Institute of Plasma Physics,the Chinese Academy of Sciences, Hefei 230031)

Abstract Superconducting TF and PF coils have been measured in SULTAN test facility. Segregated copper strands are included in four NbTi CICC and this is a technical innovation. Two AC losses measurement methods, calorimetric and electromagnetic methods, have been used in the experiments, and a broad frequency range (from 0.05 Hz to 6 Hz) is covered in sample test. The purpose of this experiment was to investigate AC losses of TF and PF CICC conductor including segregated copper and to check the design of PF and TF CICC coated with different resistive barriers (Pb–30Sn-2Sb and Ni plating on NbTi strands).

Keywords Cable-in-conduit conductor, Coupling loss time constant, Sn and Ni plated conductor, Contact resistance

CLC number TM249.7

1 Introduction

In the design of superconducting conductors of HT-7U Tokamak, AC losses of CICC are important aspects and the main contribution to the AC losses in CICC are inter-strands coupling loss and hysteresis loss. Measurements of the AC losses in NbTi CICC are important for design of HT-7U TF and PF conductor for fusion device [1] because magnetic field changes rapidly during plasma disruption and plasma initiation. CICCs show low AC losses as resistive barriers are interposed between the strands. The lower AC losses are encountered in cables constructed with strands coated by higher resistance layer and current transfers difficultly when quenching occurs. Such conductor's stability is surprisingly low. It is clear that resistance between strands must be moderate and current can transfer between strands for the stability of CICC. A good compromise between low AC losses and good stability can be determined when moderate inter-strand and inter-sub-cable barrier resistance is selected. From measurements of AC losses performed on Sn and Ni plated NbTi with different coating conductors, one can tell which is more suitable to be used in HT-7U. Meanwhile, AC losses measurements confirm the role played by the steel spacers in the losses reduction.[2]

2 NbTi cable-in conduit conductors

Two hairpin shaped samples (Sample 1 and Sample 2), made of four NbTi cable-in-conduit conductors, will be used in the HT-7U superconducting magnets. The surface of all strands are coated with a Pb-30Sn-2Sb layer of 3 μm thick for TF and PF1 conductors and are plated by a Ni layer of 2 μm thick for PF2 and PF3 conductors. The third stage sub-cables of PF1 and PF2 are only wrapped with 70% coverage by stainless steel foil of 0.05 mm thick. The last cabling stage is formed by five pieces of the thirds stage sub-cables around a copper cable core (CCC). The final cables are wrapped by stainless steel tape of 0.1 mm thick. All conductors have

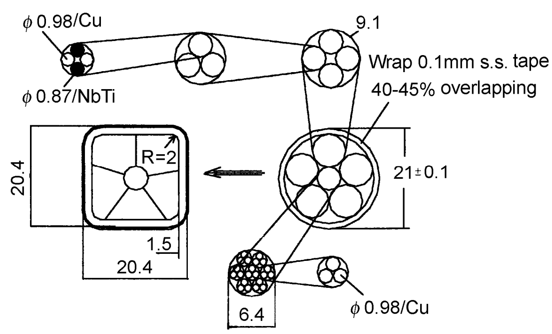

Fig. 1 The HT-7U TF and PF CICC configuration.

Received date: 2002-04-16

same cabling configuration: (2 superconducting strands + 2 copper strands) ×3×4×5 and are shown in Fig.1. Major parameters of the strand and cable are shown in Table 1 and Table 2.

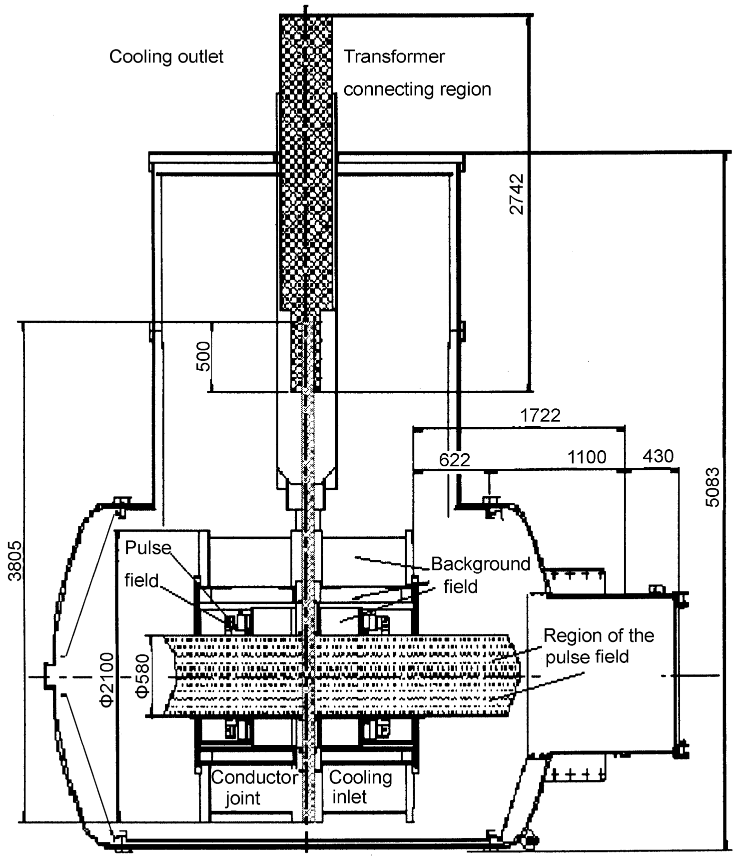

Fig. 2 Side view of the SULTAN facility.

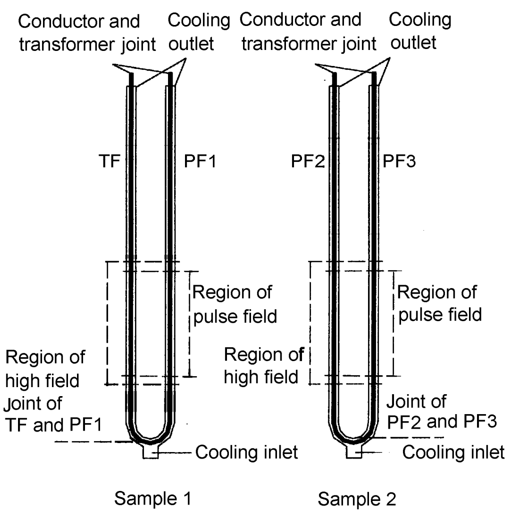

Fig. 3 Main SULTAN sample boundary conditions.

Table 1 The parameters of NbTi strand

Strand diameter(mm)	0.87
Cu/Sc[(1)]	1.38
Number of filament	8910
Filament diameter (μm)	6
Filament pitch (mm)	10
RRR	100
Thickness of Pb-30Sn-2Sb (μm)	2
Thickness of Ni (μm)	3

[(1)]Sc = Superconducting

Table 2 The description of Sample 1 and Sample 2

Conductor	Cable pattern	No. of NbTi strands	No. of Cu strands	Twist pitches (mm)	Coating	Void fraction (%)
TF	(2Sc+2Cu) ×3×4×5	120	141	50/86/117/200	Solder	37.32
PF1	(2Sc+2Cu) ×3×4×5	120	141	40/86/117/260	Ni	36.67
PF2	(2Sc+2Cu) ×3×4×5	120	141	40/86/117/260	Ni	36.67
PF3	(2Sc+2Cu) ×3×4×5	120	141	40/86/117/260	Ni	38.44

3 AC losses measurement of NbTi CICC

Two samples of HT-7U CICC conductor are put into the SULTAN bore with DC magnetic field up to 11T and DC operating current up to 100 kA, see Fig.2. A system of pulsed field coils provides the transverse pulse field for stability and the AC losses measurement experiments. Sample 1 and 2 are short in length, hairpin shaped NbTi cable-in-conduit conductors, see Fig.3. Sample1 consists of one TF conductor and one PF1 conductor (connecting TF to PF1 on joint). Sample 2 consists of PF2 and PF3 conductors (connecting PF2 to PF3 on joint). The two samples separately made of NbTi conductors with Sn and Ni plated strands will be used for comparative test of AC losses and stability behavior.

Four pieces of the jacketed conductor described above are tested in a background DC field (B_{ac}=2-6.6T) and a set of saddle shaped copper windings (i.e. pulse field coil), extend over an effective length of 390mm. Pulsed field can be used to explore the AC losses in PF and TF CICC. The amplitude of the pulsed field is set to ±0.1 T or ±0.2 T and the pulse field direction is perpendicular to both the background DC field and the current direction.

The coolant pressure on inlet of cooling channel of HT-7U TF and PF conductors is 1 MPa. The operating mass flow rate is set in the range of 2 to 5 g/s in order to reproduce the coolant speed in HT-7U PF and TF conductor (about 2.8 g/s on HT-7U conductor). For a correct extrapolation to the HT-7U operating field,[3] a number of background field will be used, e.g. 3, 3.5, 4, 4.5, 5, 5.8, 6 and 6.6 T. In the experiment under pulsed field sweep, the temperature increases to establish steady state temperature profiles. The AC losses, E, is measured by gas flow calorimetry and is evaluated from the increase of the coolant temperature ΔT, the helium specific heat C_p, the helium mass flow rate $\mathrm{d}m/\mathrm{d}t$, AC field frequency f and the cable volume V. The AC losses per cm^3 and per cycle of CICC is E:

$$E = \frac{\Delta T C_p \,\mathrm{d}m/\mathrm{d}t}{fV} \quad [\mathrm{J/m^3}] \qquad (1)$$

The coolant temperature was measured with temperature sensors attached to the cooling pipes and conductors. ΔT is deduced from the figure which shows downstream and upstream temperature under pulse field region. When the downstream temperature of the pulse field heating coolant is stable, ΔT is equal to the difference of downstream temperatures, i.e the stable temperature minus the starting temperature before rising (shown in Fig.4). When the downstream temperature of the pulse field heating coolant isn't stable (shown in Fig.5), ΔT is equal to the difference between downstream and upstream temperature (shown in Fig.6, Fig.7 and Fig.8).

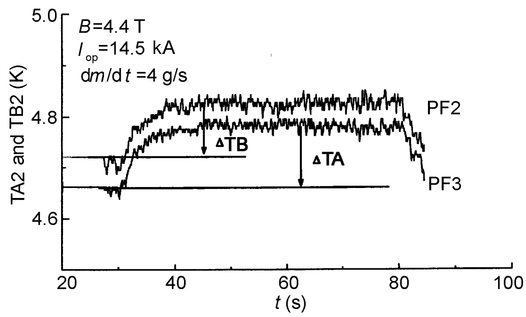

Fig.4 The downstream temperature of PF2 and PF3 under pulse field vs time. TB2: downstream tem. of PF2 under pulse field; TA2: downstream tem. of PF3 under pulse field.

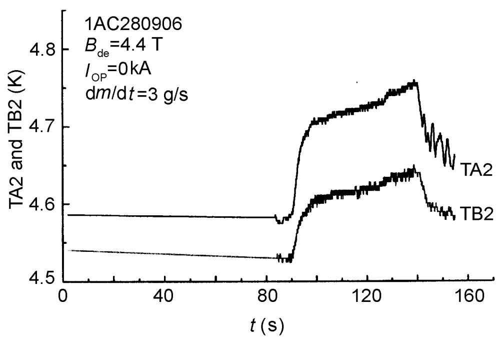

Fig.5 The downstream temperature of TF and PF1 under pulse field vs time. TA2: downstream tem. of TF under pulse field; TB2: downstream tem. of PF1 under pulse field.

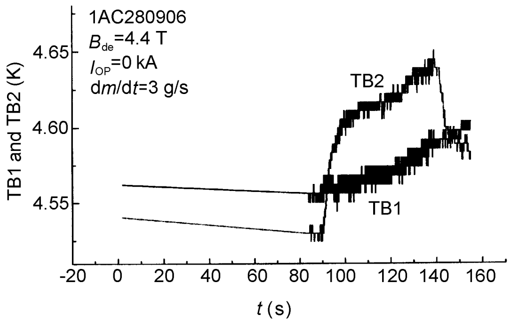

Fig.6 The upstream temperature TB1 and downstream temperature TB2 of PF1 under pulse field vs time. TB1: upstream tem. of PF1 under pulse field; TB2: downstream tem. of PF1 under pulse field.

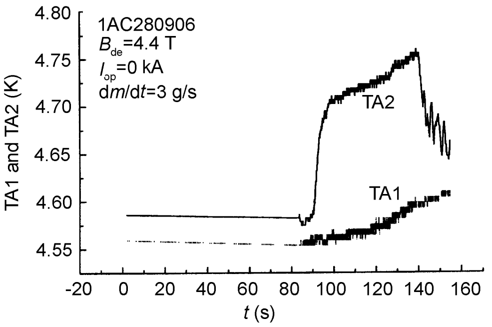

Fig.7 The upstream temperature TA1 and downstream temperature TA2 of TF under pulse field vs time. TA1: upstream tem. of TF under pulse field; TA2: downstream tem. of TF under pulse field.

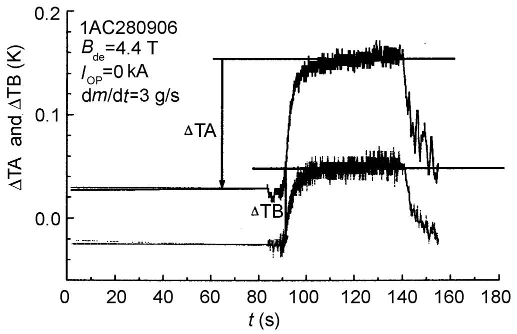

Fig.8 Difference of downstream and upstream temperature of TF and PF1 under pulse field.

When the heat slug caused by the AC losses in CICC has the shape of a trapezium, downstream temperature increase of the coolant, ΔT, is sensed by a temperature sensor placed just after the pulse field. The temperature increase of the coolant in PF2 and PF3 CICC, ΔT, can be got from Fig. 4 in this way (i.e. ΔT is equal to height of the trapezium in temperature curve).

There is not a flat top in Fig.5 for downstream temperature curve of TF and PF1 conductors (i.e. the temperature curve is not shaped like a trapezium). This situation may be caused by joint joule heat and AC losses in front of AC field. We can get ΔT by measuring the difference between the temperatures sensed by sensors placed just after the pulse field and just before the AC field (shown in Fig. 6 and Fig. 7). We do so in order to remove joint joule heat and AC losses in front of pulse field from total AC losses and get AC losses of conductor under pulse field. ΔT of TF and PF1 conductors is shown in Fig. 8,which is deduced from Fig. 6 and Fig. 7. Exactly, ΔTB in Fig. 8 is deduced from Fig. 6 and ΔTA from Fig.7 (ΔTB = TB2-TB1 for PF1, ΔTA = TA2-TA1 for TF).

It is difficult to measure change of temperature with gas flow calorimetry at low frequency AC field. When frequency of AC field is low, magnetization measurement must be taken instead of gas flow calorimetry. There are always background voltages induced in the pick up coil which must be balanced out, using a compensation coil before a magnetization measurement can be made. One can measure the area of a hysteresis loop on M-H curve to get AC losses. However, a simpler method is to measure the area of a hysteresis loop of voltage-B curve. The area is proportional to the AC losses during a cycle (see Fig. 9). Then area of the magnetization loop is calibrated against the calorimetric values at the same frequency. For example, at 0 transport current, AC losses are measured at five frequencies (2, 3, 4, 5 and 6 Hz) by calorimetric methods, and areas of the magnetization are measured at seven frequencies (0.05, 0.1, 0.5, 0.8, 1, 2 and 3 Hz) by magnetization methods. One can apply results measured at 2 Hz and 3 Hz by calorimetric methods to calibrate the result of magnetization at same frequencies because magnetization loop (integrate of voltage–B) measures the fraction of AC losses at low frequencies.

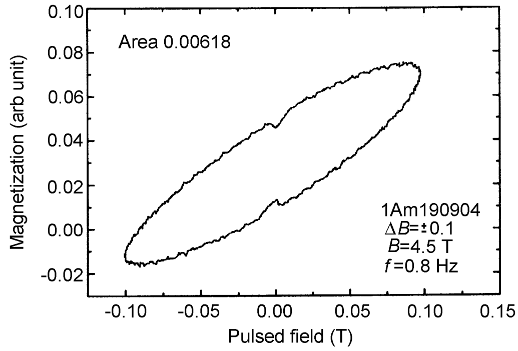

Fig.9 Magnetization loops (vertical axis represents the integrate of voltage –pulse field) of PF1 at 0.8 Hz.

In order to make question simply, magnetization method without carrying current is used and the accuracy of the AC losses measurement is about 2 %.[4]

4 Measurement results and analysis

The losses results of PF1 and TF conductor have been got by magnetization (by pick-up coil) and gass-flow calorimetry. The tests were carried out at 1MPa and 4.5-6 K. Pulse field is perpendicular to sample axis (sample is straight except connection). The AC losses were measured for sinusoidal cycle from -0.1 to +0.1 (ΔB = 0.1 T) or –0.2 to +0.2 (ΔB = 0.2 T). The frequency ranges of pulse field were covered from 0.05 to 3Hz for electrical magnetization measurements and from 2 to 6 Hz for gass-flow calorimetry. Gass-flow calorimetry was used to calibrate the magnetization loops, which offers a better accuracy at low field rates. The pulsed field coil spans 390 mm of conductor. According to Table 1, two coatings have been investigated on NbTi strands for contact resistance, in the frame of the CICC development for superconducting Tokamak magnets, including Ni and Pb-30Sn-2Sb. An important parameter that determines the coupling AC losses in superconducting cables is the inter-strand resistance. We measured to-

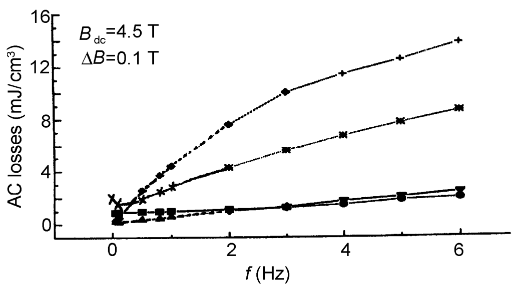

Fig.10 AC losses curves of TF, PF1, PF2 and PF3 conductors without carrying current with pulse field $\Delta B = \pm 0.1$T (peak-to-zero field) and background field B_{dc}=4.5T. ■ PF3 magnetization; ● PF3 calorimetry; ▲ PF2 magnetization, ▼ PF2 calorimetry; ◆ TF magnetization; + TF calorimetry; × PF1 magnetization; ＊PF1 calorimetry.

tal AC loss energy per unit of cable and cycle generated by transverse sinusoidal field.

The AC losses were plotted as a function of frequency of the AC field. Measurement was performed on four prototype conductors for HT-7U and results with background field B_{dc} = 4.5T and without current are shown in Fig.10. In the course of experiment, ΔB was 0.1T and magnetization measurements from 0.05 to 3 Hz were calibrated by gas-flow calorimetry from 2 to 6Hz. As a result, the figure of AC losses from 0.05 to 6 Hz was obtained.

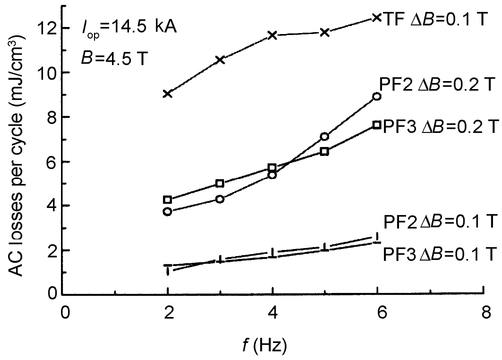

Fig.11 AC losses curves of TF, PF1, PF2 and PF3 conductors with carrying current.

The results of AC losses with background field B_{dc} = 4.5T and with current I_{op} = 14.5 kA are shown in Fig.11, with ΔB being 0.1T or 0.2T. The gas-flow calorimetry measurement curves from 2 to 6 Hz show that AC losses increase as ΔB increases. In Sn coated cables, larger coupling time constants exist in Sn coated cables (TF and PF1) and lower coupling time constants exist in Ni coated cables (PF2 and PF3) as the Ni coating effectively cuts the inter-strand loops.

The coupling loss per unit volume of cable per cycle increases linearly with frequency and the square of amplitude of magnetic field ΔB [5]:

$$Q_c = \frac{\pi n\tau\omega\Delta B^2}{\mu_0(\omega^2\tau^2+1)} \approx \frac{\pi n\tau\omega\Delta B^2}{\mu_0} \quad [\mathrm{J/(m^3 \cdot cycle)}] \tag{2}$$

The applied field $B = \Delta B \sin \omega t$, and the effective coupling current time constant $n\tau$ is decided by ΔB and the slope α of the linear section of Q_c at low frequency :

$$n\tau = \frac{\alpha\mu_0}{2\pi^2\Delta B^2} \quad [\mathrm{s}] \tag{3}$$

Parameters of the strands used for the comparison action of coating are listed in Table 1. The coupling time constant $n\tau$ of TF, PF1, PF2 and PF3 are listed in Table 3.

Because of the non-linear behavior of TF, PF1, PF2 and PF3 conductors, their $n\tau$ values are obtained from the initial slope of the losses curve (f~0.05-0.1 Hz).

The Ni coating has been proved to be effective to cut the inter-strand loss in PF2 and PF3 CICC. Both PF2 conductor with Ni coating and petal wraps and PF3 conductor have low AC losses and $n\tau$ values. The petal wraps is not necessary for cutting the inter-strand losses as Ni plated strands indicate almost one order of magnitude higher resistance than those Sn-plated.

Contact resistance R_c can be calculated with [6]:

$$R_c = \left[\frac{n\tau}{k \cdot 5.53 \cdot N}\right]^{-1.54} \quad (4)$$

where N is total number of strands including the pure copper strands, k = 0.3 for a full-size conductor with petal-wraps and k = 0.7 for a full-size conductor without petal-wraps.

Table 3 Coupling time constant $n\tau$ of TF, PF1, PF2 and PF3

Conductor	TF	PF1	PF2	PF3
Coupling time constant $n\tau$ (ms)	36.79	13.45	2.31	5.1

There is consensus about a 100-200 nΩ·m criterion with respect to stability performance of TF and PF conductors. When resistance of coating is below 100-200 nΩ·m, current can transfer between strands easily and stability of cable is satisfactory. Meanwhile, lower AC losses require larger resistance between strands, and limiting $n\tau$ to 100 ms is required for lower AC losses.

For $n\tau$ = 36.79 ms in an NbTi TF CICC without petal-wraps, an R_c value of 164.3 nΩ·m is predicted from formula (4). If the last stage petals of PF1 are wrapped with high resistance stainless steel foil, then an R_c of 210.0 nΩ·m is predicted. R_c of PF2 and PF3 are larger than 100 nΩ·m and they are not appropriate candidates. Contact resistance values R_c of TF, PF1, PF2 and PF3 are listed in Table 4. The Sn coating has very low contact resistance and is not recommended for low loss cables. But, a full size PF1 conductor with Sn coating and petal wraps in last sub-cable produces a very low AC losses and can be applied to HT-7U PF and TF coil.

According to formula (4), N and R_c will increase with the inclusion of copper strands in the cable and the coupling loss will decrease. When quenching occurs, current will flow into copper strands. Therefore copper strands can improve stability of CICC. On the other hand, the fact that copper strands can increase cooling perimeter becomes another reason for the high stability of CICC.

Table 4 Contact resistance R_c of TF, PF1, PF2 and PF3, according to formula (4)

Conductor	Coupling loss time constant (ms)	Contact resistance R_c (nΩ·m)
PF1	13.45	210.0
TF	36.79	164.3
PF2	2.31	3164.0
PF3	5.1	3445.2

In the full size PF2 and PF3 conductors, the losses increase when a stationary transport current flows. The increase of losses may originate from the transport current loss or self-field loss, the enhanced inter-strand coupling loss due to Lorentz force working on the contacts in CICC. Meanwhile, the saturation or screening of a cable reacts to coupling loss and restrains the increase in coupling loss. See Fig.12.

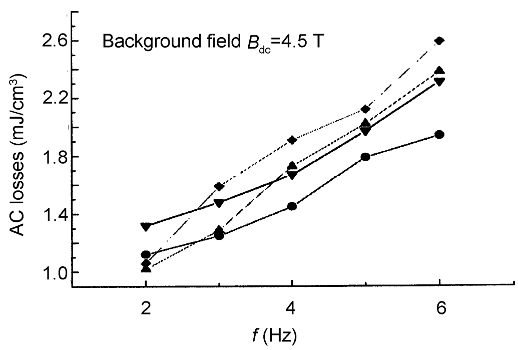

Fig.12 The AC losses curves of PF2 and PF3 conductors with or without current. ● PF3 without current; ▲ PF2 without current; ▼PF3 with current; ◆ PF2 with current.

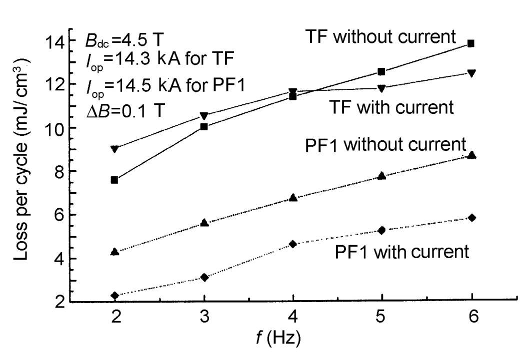

Fig.13 The AC losses curves of TF and PF1 conductors with or without current.

But, in the full size TF conductor, the losses hardly increase when a stationary transport current flows. On the other hand, the losses of PF1 decrease when a stationary transport current flows. This effect is mainly attributed to the superconducting properties of the Pb-30Sn-2Sb. In TF and PF1 CICC with solder coatings, resistance of Sn will increase when a stationary transport current flows and magnetic field increases. Resistivity of Sn is very low and when TF and PF1 carry current, screening is stronger and AC losses are much lower. Meanwhile, when magnetic field increases due to current in conductor, the magnetoresistance effect on copper matrix appears and losses decrease. This explains the situation in Fig.13.

5 Conclusion on AC losses

The coupling current losses in Ni and Sn plated NbTi CICC present a complex behavior, i.e. there is a minor loss peak at very low frequency ($f < 0.03$ Hz). This minor loss peak may be due to the large current loop in inter-strand, which may be associated to larger time constant. Meanwhile, it must be noticed that large current loops are restricted to a limited cable volume and AC losses are not too large.

Four conductors show unexpected non-linear behaviour in the losses versus frequency curve. Coupling losses time constants and hysteresis loss are determined from the initial slopes and linear section of the curve for all HT-7U CICCs.

We have measured the coupling losses time constants on four NbTi CICCs with segregated copper strands with Ni and Sn surface coatings. The TF CICC with Sn coatings produces the highest coupling losses while Ni plated PF3 conductor shows the lowest coupling losses. Though PF1 with Sn coatings has the same configuration as TF, time constant of PF1 is only half that of TF as its third stage sub-cables are wrapped with 70% coverage by stainless steel foil of 0.05mm thick.

The empirical relation (4) for R_c and $n\tau$ can be applied to the design of a full size CICC. We measured AC losses of CICC and got the $n\tau$ values of TF and PF1 ($n\tau$ for TF and PF1 is 36.79 ms and 13.45 ms respectively). Formula (4) can be used for the calculation of R_c if $n\tau$ is given. So, petal-wraps are required in third sub-cable. Though Ni plated PF2 and PF3 show very low inter-strand coupling loss in the range of about 2-5 ms, R_c for PF2 and PF3 are too high to transfer current between strands and sub-cable and stability can not be kept.

In the third stage sub-cables of PF1 CICC with petal-wraps, current can be transferred between strands and sub-cable and stability can be kept.[7] Meanwhile, steel spacer plays a role in the cutting large current loops and perhaps PF1 is more suitable to use in HT-7U.

Every cooling channel in HT-7U superconducting Tokamak PF coil [8] is about 140-170 m long if we select PF1 as PF conductor. Coupling losses will increase the coolant temperature to less than 0.2 K, when plasma initiation and disruption occur. Though the measurement on a short CICC was not able to predict AC losses in a large coil, we have got much more valuable information still.

Acknowledgment

The authors thank Dr. P. Bruzzone for his help with theoretical analysis and AC loss measurement. The authors also thank PSI institute in Switzerland to supply experimental facility.

References

1 Weng P D, Bi Y F, Chen Z M *et al.* Cryogenics, 2000, **40**: 531-535

2 Ciazynski D, Turck B, Duchateau J L *et al.* IEEE Appl Supercon, 1993, **1**: 594-601

3 Fang J, Chen Z M, Wu S T *et al.* Plasma Sci and Technol, 2000, **4**: 383-396

4 Bruzzone P, Nijhuis A. IEEE Appl Supercon, 2001, **11**: 2018

5 Fang J, Chen Z M, Li B Z *et al.* Plasma Sci and Technol, 2000, **6**: 549-556

6 Nijhuis A, Morsink E. Contact resistance and coupling loss in NbTi CICC's with different strand coatings produced by Jcs VNIIKP(RU), 1st Intermediate Report, UT-NET /EFDA 2001-3, contract No.: EFDA-01/XXX, Task 1&2, April 12, 2001

7 Nijhuis A. Control of contact resistance and coupling loss by strand surface coating in sub-size NbTi CICC's, Final Report UT-NET/EFDA 2000-6, contract No.: NET/98-479, Task 3B, December 21, 2000 (and the intermediate report for EFDA-99/503 Task 1C)

8 Weng P D, the HT-7U team. The engineering design of the HT-7U Tokamak, Proceedings of the 21st Symposium on Fusion Technology, 2001, **58-59**: 827-831